IL NUOVO CIMENTO Vol. 34 C, N. 4 Luglio-Agosto 2011
DOI 10.1393/ncc/i2011-10952-4

Colloquia: Channeling 2010

Electromagnetic radiation accompanying multiple volume reflection in one crystal

V. Guidi(1), A. Mazzolari(1) and V. V. Tikhomirov(2)(*)

(1) *Dipartimento di Fisica dell'Università and INFN, Sezione di Ferrara - Ferrara, Italy*
(2) *Research Institute for Nuclear Problems, Belarus State University - Minsk, Belarus*

(ricevuto il 22 Dicembre 2010; pubblicato online il 29 Agosto 2011)

Summary. — An interpretation of the first experiment on gamma-radiation of 120 GeV positrons experiencing multiple volume reflection from planes of one bent crystal is given. An increase of radiation of 10–20 GeV gamma quanta by multiple reflection from skewed planes is demonstrated. Also a considerable influence of the axial field on both hard and soft parts of the positron radiation spectrum is revealed.

PACS 41.60.-m – Radiation by moving charges.
PACS 52.38.Ph – X-ray, γ-ray, and particle generation.
PACS 61.85.+p – Channeling phenomena (blocking, energy loss, etc.).
PACS 41.75.Ht – Relativistic electron and positron beams.

1. – Introduction

As is widely known, coherent particle scattering in crystals is accompanied by specific effects in radiation, such as the coherent bremsstrahlung and channeling radiation. The volume reflection (VR) effect [1], widely investigated last years, is also accompanied by some radiation process [2] already observed experimentally [3], which manifests itself in a wider angular interval than both the coherent bremsstrahlung and channeling radiation.

Recently the possibility to observe multiple VR from different plane sets of one crystal (MVROC) was predicted [4] and a five-time increase of the proton deflection angle by the succesive VR from different planes intersecting along the $\langle 111 \rangle$ Si axis was observed experimentally [5, 6]. An increase in particle deflection by MVROC has naturally led to the same phenomenon in radiation intensity. An interpretation of the first results of the experimental investigation of positron radiation accompanying the MVROC [7] is given.

(*) E-mail: vvtikh@mail.ru

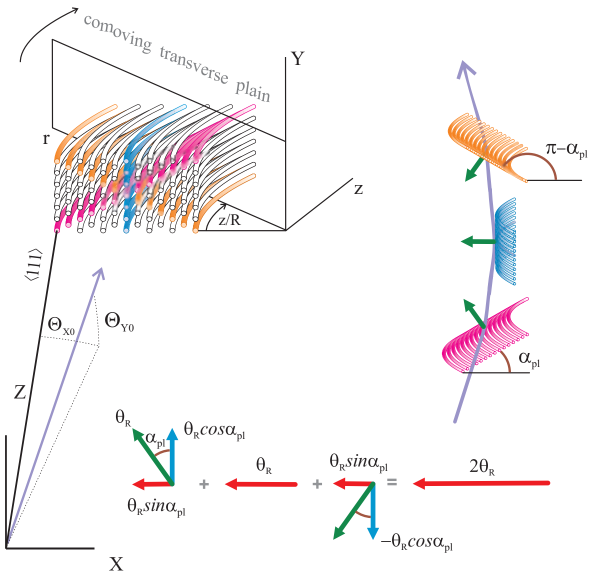

Fig. 1. – Particles which hit a crystal at small angles Θ_{X0}, Θ_{Y0} with respect to crystal axes, like $\langle 111\rangle$, experience VR from both the "vertical", $(1\bar{1}0)$, and numerous skew planes, like $(\bar{1}01)$ and $(0\bar{1}1)$. Horizon projections of the angles of reflection from different skew planes sum up giving rise to the MVROC effect while the vertical angles of reflection from symmetric skew planes, like $(\bar{1}01)$ and $(0\bar{1}1)$, mutually compensate. Comoving reference system rYz rotates with the bent axis direction when a particle moves through the crystal.

2. – Particle motion under MVROC

VR occurs when a particle trajectory becomes tangential to a bent crystalline plane. Since a crystal axis is parallel to the line of intersection of various crystal planes, reflection from most of them will arise as a proton moves at a small angle with respect to such an axis [4]—see figs. 1 and 2.

Figure 2 also illustrates the evolution of the vertical ψ_Y and horizontal ψ_r particle deflection angles in the reference system rYz, comoving with a particle channeled with

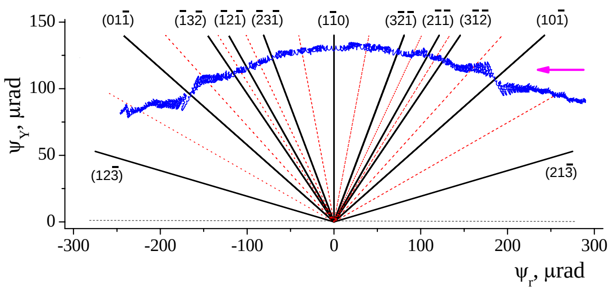

Fig. 2. – Particle trajectory against a background of crystal planes intersecting along the $\langle 111\rangle$ axis (solid) and the regions of the influence of the latter (dashed) under the conditions of the experiment [7].

zero transverse momentum along bent $\langle 111\rangle$ crystal axes. Initial values of the angles ψ_r and ψ_Y are equal to the particle incidence angles Θ_{X0}, Θ_{Y0} with respect to the crystal axis at the entry face of the crystal. Since the angle ψ_r decreases with z because of the crystal bending, the vector $\boldsymbol{\psi} = (\psi_r, \psi_Y)$ becomes subsequently parallel to the different planes intersecting along the axis. The particle interaction with each of them is accompanied by VR to the direction perpendicular to the plane at the tangency point and opposite to the crystal bending axis.

The reflection from skew planes gives deflection in both horizontal and vertical directions. Deflection angles are $\theta_X = -\theta_R \sin\alpha_{pl}$ and $\theta_Y = \theta_R \cos\alpha_{pl}$, where α_{pl} is the inclination angle of the plane and θ_R is the deflection angle for a single VR from a plane with bending radius $R/\sin\alpha_{pl}$—see fig. 1. Since $\sin\alpha > 0$ for any $0 < \alpha < \pi$, all the horizontal deflection angles θ_X sum up providing a deflection to the same direction. On the contrary, since $\cos(\pi-\alpha) = -\cos\alpha$, the vertical deflections accompanying the reflection from symmetric skew planes with complementary inclination angles α_{pl} and $\pi - \alpha_{pl}$ mutually compensate each other. Thus, if the horizontal incidence angle and the crystal bending angle $\varphi = l/R$ satisfy the condition

$$\Theta_{X0} = \varphi/2, \tag{1}$$

all skew planes will be involved in the VR process by symmetrical pairs, as figs. 1 and 2 illustrate, allowing to reach nearly zero net vertical deflection.

In order to reach a really considerable deflection angle, it is necessary to involve the strongest skew planes in the reflection process. Figure 2 shows that skew planes involved in the reflection process are the ones with inclination angle α_{pl} not exceeding the value $\alpha_{\text{inc}} = \arctan(\Theta_{Y0}/\Theta_{X0})$ of the inclination angle of the particle incidence plane to the axis. Equation (1) allows to write this condition in the form

$$\varphi > 2\Theta_{Y0}\cot\alpha_{pl}. \tag{2}$$

According to eq. (2), the strongest inclined planes $(\bar{1}01)$ and $(0\bar{1}1)$ intersecting along the $\langle 111\rangle$ axis are involved in reflection provided that $\varphi > 3.46\Theta_{Y0}$. Finally, effective particle reflection from main crystal planes formed by crystal axes becomes possible when the vertical incidence angle Θ_{Y0}, simultaneously playing the role of the minimal angle of particle motion with respect to the crystal axis, exceeds the axial channeling angle at least two-three times.

The described conditions of effective MVROC were satisfied in the first MVROC radiation experiment conducted with 120 GeV positrons impinging the $\langle 111\rangle$ axis of 2 mm Si crystal bent with radius $R = 4.7$ m and angle $\varphi = l/R \simeq 426\,\mu$rad with the angles $\Theta_{Y0} \simeq 100\,\mu$rad and $\Theta_{X0} \simeq 275\,\mu\text{rad} > \varphi/2$.

3. – Planar contribution to the MVROC radiation

A typical positron trajectory is shown in fig. 2, demonstrating both the distinct reflection from the low-index skewed planes $(10\bar{1})$ and $(01\bar{1})$ and the less pronounced one from many others shown. Both soon before and after a reflection the particle experiences oscillations in the field of the reflecting set of planes. In this section we will mainly address the planar radiation caused by these oscillations. To describe the latter one should first determine the angular intervals of positron motion with respect to the crystal planes. Let us consider the particle motion between i-th and $(i+1)$-th planes in terms of inter-axis distances $d_{ax,i}, d_{ax,i+1}$ and unit vectors $\mathbf{a}_i = (\cos\alpha_{pl,i}, \sin\alpha_{pl,i})$, $\mathbf{a}_{i+1} = (\cos\alpha_{pl,i+1}, \sin\alpha_{pl,i+1})$ specifying the directions of the crystal plane projections on the rY-plane, shown in fig. 2 by the solid lines. The vector $\boldsymbol{\psi} = (\psi_r, \psi_Y)$ specifying analogically the direction of the rY-projection of the plane separating the angular regions of influence of i-th and $(i+1)$-th planes can be determined from the equation

$$d_{ax,i}[\boldsymbol{\psi}, \mathbf{a}_i] = -d_{ax,i+1}[\boldsymbol{\psi}, \mathbf{a}_{i+1}] \tag{3}$$

following in the straight-line approximation from the condition of equality of changes of the impact parameter of particle collision with successive atomic strings from i-th and $(i+1)$-th crystal planes. Inclination angles

$$\alpha = \arctan(\psi_Y/\psi_r) \tag{4}$$

of the "transition" planes, shown by dashed lines in fig. 2, allow to introduce the maximum angles

$$\theta_{i,i+1} = \psi \sin(\alpha - \alpha_{pl,i}) \tag{5}$$

of the particle motion under the influence of the i-th plane. Since these angles depend on the angle ψ of particle motion with respect to the crystal axis, they were averaged over many particle trajectories simulated using the method [6]. Simulations were also used to obtain averaged lengths l_i of particle motion in the regions of influence of each of the planes shown in fig. 2. The averaged values $\langle\theta_{i,i+1}\rangle$ and $\langle l_i\rangle$ were further used to evaluate the spectrum of radiation induced by oscillations in the field of different plane sets.

The character of radiation process is in general determined by the ratio of particle deflection angle and the typical radiation angle by ultra-relativistic particles $1/\gamma$ equal to $4.3(8.5)\,\mu$rad at $\varepsilon = 120(60)$ GeV. The angle of particle deflection both before and after VR is determined by the channeling angle ϑ_{ch} reaching $19(27)\,\mu$rad at 120 (60) GeV and, thus, exceeding $1/\gamma$ at least three times. Even at the highest possible angles $\theta = \theta_{i,i+1} \simeq 50\,\mu$rad of positron motion with respect to main crystal planes (110) the deflection angle remains close to $1/\gamma$.

In cases when the particle deflection angle exceeds $1/\gamma$ its radiation attains a synchrotron-like nature. However if this excess is not large, as in our case, the simple formulae describing radiation in the uniform field cannot be used and a direct radiation characteristic evaluation using the Baier-Katkov formula (BKF) [9] should be undertaken. The most efficient and general method to conduct such calculations in the case of planar motion was developed in [8] on the basis of both a special BKF representation and Fast Fourier transform method [9]. The approach of [8] as well as the averaged values $\langle\theta_{i,i+1}\rangle$ and $\langle l_i\rangle$ for the crystal planes depicted in fig. 2 were used to evaluate the spectral radiation intensity distributions in the field of those planes (fig. 3). These distributions demonstrate that the main contribution comes from the major skewed planes $(10\bar{1})$ and $(01\bar{1})$. Namely the four-fold excess of their contribution over that from the "vertical" plane $(1\bar{1}0)$ is reached due to the simultaneous doubling of both the plane number and time (length l_i) of positron oscillations in the field of each of the planes related with their inclination. The small values of the contributions of the other higher-index planes to the radiation intensity are explained by both the lower oscillation amplitudes and durations.

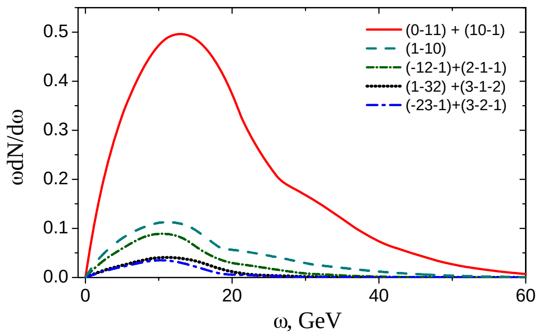

Fig. 3. – Contribution of different plane sets to radiation spectral intensity.

Summed over all the planes radiation intensity spectra of positrons with energies $\varepsilon_0 = 120$, 100 and 80 GeV are shown in fig. 4. Note that the heights of all these spectra practically coincide and all three of them are geometrically similar provided the photon energy scale is squeezed with positron one like $\varepsilon_0^{1.75}$. Such a favorable behavior allows to use these spectra to interpolate the radiation probability for an arbitrary positron energy from the experimental interval [7] 60 GeV $\leq \varepsilon \leq$ 120 GeV and to apply it to the simulations of the observed positron energy loss spectra.

Figure 4 also allows to compare the 120 GeV positron radiation in the MVROC and VR cases in the same crystal with 2 mm length and 4.7 m bending radius. Much harder spectrum in the latter is explained by the larger possible angles $\theta \sim \varphi/2$ of the positron motion with respect to the "vertical" plane $(1\bar{1}0)$. These larger angles make the radiation of positrons oscillating in the planar field harder in two ways at once. Namely, they make, first, the oscillation period shorter and, second, the oscillation amplitude smaller increasing by this the average positron velocity and facilitating this way the Doppler blue shift of the oscillator radiation. Nevertheless, though the single VR geometry increases the hard photon emission, we will show now that the axial influence on positron motion in the MVROC geometry facilitates the hard radiation even stronger.

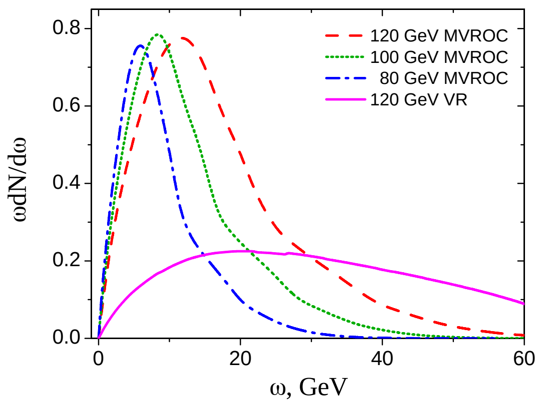

Fig. 4. – Spectra of radiation of 120, 100 and 80 GeV positrons in MVROC conditions and of 120 GeV positrons in VR conditions, all in 2 mm Si crystal bent with radius of 4.7 m.

4. – Axial contribution to the MVROC radiation

A particle scattering by crystal axes is inherently connected with the MVROC process. To make the latter efficient, a minimal value Θ_{Y0} of the angle ψ of particle motion with respect to crystal axis should be less than half a crystal bending angle (see eq. (2)), which in turn is limited by both crystal length value and the necessity to use relatively large crystal bending radii for an efficient VR. Since the radiation intensity increases fast with ψ decrease, a limited ψ value predetermines a considerable contribution of the axial field to the radiation accompanying MVROC.

A theoretical study of particle radiation in the field of atomic strings constituting crystal planes was started in [10]. Both coherent bremsstrahlung (CB) and synchrotron-like approximations were used in the latter. At the same time the maximum angle $\psi \simeq V_0/\psi\varepsilon, V_0 \simeq 106\,\text{eV}$, of positron deflection in the field of an $\langle 111\rangle$ Si axis, in fact, reaches $1/\gamma$ and exceeds that in Ge allowing to use the CB theory, possibly modified by the uniform field influence, only for a qualitative description of the axial contribution to the MVROC radiation making necessary a direct BKF evaluation for a quantitative one. Here we suggest some elementary but efficient modification of the method of such calculations undertaken for the first time in [11]. Namely, a direct integration by parts allows to represent the typical BKF integral in the form

$$\begin{aligned}(6)\qquad &\int_{t_1}^{t_2} \exp\left[i\frac{\omega\varepsilon}{2\varepsilon'}\int_{-\infty}^{t}\left[\gamma^{-2}+(\mathbf{v}_\perp(t')-\boldsymbol{\theta})^2\right]\mathrm{d}t'\right]\mathrm{d}t \\ &= \frac{2\varepsilon'}{i\omega\varepsilon}\frac{1}{\gamma^{-2}+(\mathbf{v}_\perp(t)-\boldsymbol{\theta})^2}\exp\left[i\frac{\omega\varepsilon}{2\varepsilon'}\int_{-\infty}^{t}\left[\gamma^{-2}+(\mathbf{v}_\perp(t')-\boldsymbol{\theta})^2\right]\mathrm{d}t'\right]\Bigg|_{t_1}^{t_2} \\ &+\int_{t_1}^{t_2}\frac{2\varepsilon'}{i\omega\varepsilon}\frac{\mathrm{d}\mathbf{v}_\perp(t)}{\mathrm{d}t}\frac{2(\mathbf{v}_\perp(t')-\boldsymbol{\theta})}{\left[\gamma^{-2}+(\mathbf{v}_\perp(t)-\boldsymbol{\theta})^2\right]^2}\exp\left[i\frac{\omega\varepsilon}{2\varepsilon'}\int_{-\infty}^{t}\left[\gamma^{-2}+(\mathbf{v}_\perp(t')-\boldsymbol{\theta})^2\right]\mathrm{d}t'\right]\mathrm{d}t,\end{aligned}$$

separating this way the contributions of the initial t_1 and final t_2 points of the arbitrary trajectory interval $[t_1, t_2]$. We suggest here to omit these contributions, thus both neglecting the contribution of the "end" effects to radiation and drastically improving the convergence of the radiation intensity integral over the photon emission angles $\boldsymbol{\theta}$.

Direct BKF integration over both time and photon emission angles allows to investigate numerically the general case of photon emission by positrons experiencing scattering by atomic strings arranged in planes. In reality a limited number of periods (say, four) of the planar above-barrier oscillations was used in calculations, while the results were normalized to the 2 mm experimental crystal thickness. Spectral distributions of radiated intensity in the field of the strong (110) plane at $\theta = 20\,\mu$rad and $\psi = 160\,\mu$rad and of a "weak" (321) plane at $\theta = 7.5\,\mu$rad and $\psi = 150\,\mu$rad are shown in fig. 5. A comparison with fig. 4 confirms the dominating role of the planar radiation in the 10–20 GeV region, though a reliable evaluation of the planar radiation peak heights needs an averaging of such spectra over all the plane sets and different positron directions of motion in the fields of the latter.

However the spectra behavior at higher photon energies demonstrates the dominant role of the field of atomic strings. A constructive interference of radiation amplitudes in the field of different strings leads to the formation of the main peaks near 45 and 30 GeV. A comparison with the predictions of the CB theory (see fig. 5 top) shows that though the latter explains both the position and, partially, the profile of the interference peaks

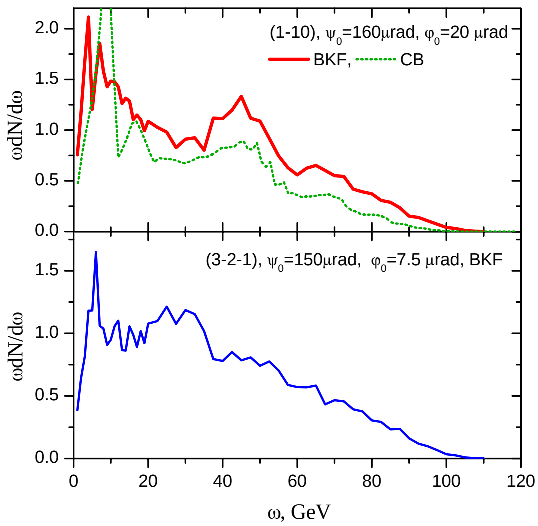

Fig. 5. – Spectra of energy radiated by 120 positrons in the 2 mm Si crystal in the field of (110) (top) and (321) (bottom) planes. CB theory predictions are also shown for the former by a dotted line.

near 45 and 65 GeV, a systematic difference of the heights of the curves demonstrates the inability of the CB theory to describe the MVROC radiation quantitatively.

The behavior of the spectra in between the "planar" and "axial" peaks is determined by a considerable interplay of axial and planar features of positron motion and cannot be treated analytically. The peaks in the soft part of the spectrum are greatly influenced by the usage of positron trajectories of limited length and should be considered as artifacts. Note only that because of the small intensity of the planar radiation the irregular positron scattering by atomic strings becomes important in this spectral region.

In general, though a direct calculation using the BKF is, in principle, possible in the considered experimental situation, evaluations of the spectra in the intervals of $\varepsilon, \omega, \theta$ and ψ variation necessary for a full-scale Monte-Carlo simulations are too time-consuming for personal computers and their parallel evaluation on the SKIF Supercomputer of BSU will be used in the near future. That is why to give a fast interpretation the first results on the MVROC radiation in the spectral region $\omega < 60\,\mathrm{GeV}$ we have chosen another approach. Namely, we modified the planar radiation spectra from fig. 4 in both hard and soft photon energy regions and used the obtained artificial spectrum shown in fig. 6 (compare with fig. 5) to simulate the experimental positron energy distribution forming under conditions of multiple photon emission, shown in fig. 7.

While both the type and scale of modification of the hard part of the emission spectrum were directly motivated by the spectra from fig. 5, that of the soft one was not so evident. Namely, we proceed from the guess that the irregularity of the positron motion in the field of different atomic strings has also to influence the soft part of the radiation spectrum. Since the radiation coherent length (and time) considerably exceeds that of a positron-string collision, the latter can be considered as not completely correlated instant kicks. Like the ones by atoms in amorphous medium such short kicks lead to the Bethe-Heitler-like spectrum $\mathrm{d}W/\mathrm{d}\omega \sim A/\omega$, the scale A of which is determined by both axial field strength and degree of correlation of positron scattering by separate strings.

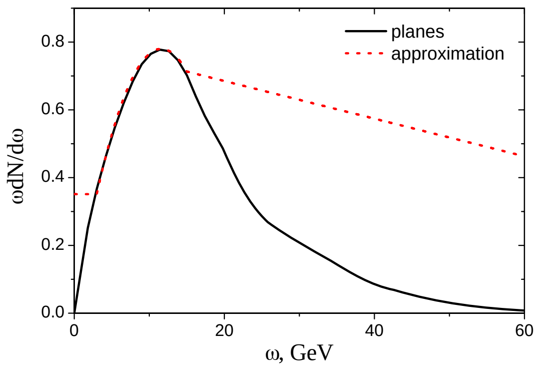

Fig. 6. – Modification of the planar radiation spectrum used to reproduce the experimental positron energy loss distribution.

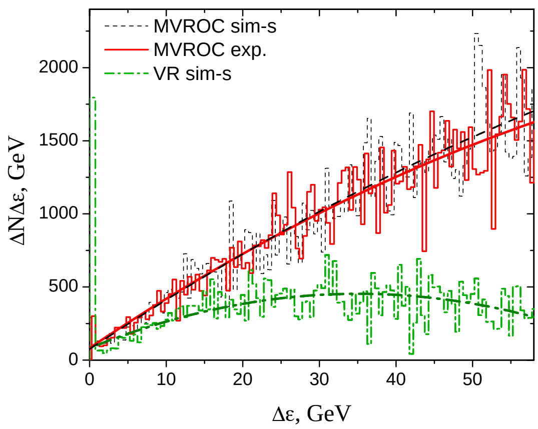

Fig. 7. – Experimental positron MVROC energy loss spectrum (solid line), simulated MVROC (dashed line) and VR (dash-dotted line) energy loss spectra. Polinomial interpolations are also shown by the same types of lines.

Since the latter is difficult to treat analytically in general, the simplest way to restore the experimental spectrum was to infer the A value from the experiment. Indeed, the value about an order of magnitude exceeding that following from the BH formula allows to simultaneously explain both the form of the soft part of the energy loss spectrum of positrons and the observed eighty percent probability of losing more than 5 GeV energy by them.

5. – Conclusions

Thus we have demonstrated that the positron radiation in the field of crystal planes dominates in the photon spectral region $10 \leq \omega \leq 20$ GeV in which the main skewed planes $(10\bar{1})$ and $(01\bar{1})$ give a 60% contribution to the total radiation intensity.

The axial field contribution to the radiation intensity becomes principally important at $\omega \geq 20$ GeV and does not strongly depend on the inclination of the plane of positron motion (the plane parallel both to the crystal axis and instant positron velocity). Coherent bremsstrahlung theory is unable to describe this type of radiation quantitatively and a new theoretical approach is required.

A chaotic component of the positron scattering by atomic strings explains the manifestation of considerable soft radiation at $\omega \leq 5\,\mathrm{GeV}$ which cannot be explained by the field of crystal planes.

REFERENCES

[1] Taratin A. M. and Vorobiev S. A., *Phys. Lett. A*, **119** (1987) 425.
[2] Chesnokov Yu. A., Kotov V. A., Maisheev V. A. and Yazynin I. A., *JINST*, **3** (2008) P02005.
[3] Scandale W. *et al.*, *Phys. Rev. A*, **79** (2009) 012903.
[4] Tikhomirov V. V., *Phys. Lett. B*, **655** (2007) 217.
[5] Scandale W. *et al.*, *Phys. Lett. B*, **682** (2009) 274.
[6] Guidi V., *J. Appl. Phys.*, **107** (2010) 114908; DOI: 10.1063/1.3407526.
[7] Hasan S. *et al.*, in *Channeling 2010, Book of Abstracts*, p. 19.
[8] Tikhomirov V. V., *Nucl. Instrum. Methods B*, **82** (1993) 409.
[9] Baier V. N., Katkov V. M. and Strakhovenko V. M., *Electromagnetic Processes at High Energies in Oriented Single Crystals* (World Scientific, Singapore) 1998.
[10] Baier V. N., Katkov V. M. and Strakhovenko V. M., *Nucl. Instrum. Methods B*, **69** (1992) 258.
[11] Tikhomirov V. V., *JETP Lett.*, **58** (1993) 166.